LA-UR- 00-3550

Title: QSAR OF DISTRIBUTION COEFFICIENTS FOR PU (NO3)062-COMPLEXES USING MOLECULAR MECHANICS

Author(s): Mary E. Barr, NMT-11; Gordon D. Jarvinen, NMT-11; Eddie W. Moody, NMT-11

Submitted to: JOURNAL of RADIOANALYTICAL and NUCLEAR CHEMISTRY - proceedings from MARC V Conference April 2000

Unclassified/Not UCNI
AUG 10 2000
LANL Class. Group date

Los Alamos
NATIONAL LABORATORY

QSAR of distribution coefficients for $Pu(NO_3)_6^{2-}$ complexes using molecular mechanics

Journal of Radioanalytical and Nuclear Chemistry
Marc V Conference
Kona, Hawaii
April 2000

E. W. Moody,*M. E. Barr, and G. D. Jarvinen

Nuclear Materials Technology Division, Los Alamos National Lab, Los Alamos, NM 87545 USA
** E- mail: emoody@lanl.gov*

Abstract

Computer-aided modeling has been very successful in the design of chelating ligands for the formation of selective metal complexes. We report herein preliminary efforts to extend the principles developed for ion-specific chelating ligands to the weaker, more diffuse electrostatic interactions between complex anions and dicationic sites of anion-exchange resins. Calculated electrostatic affinity between plutonium (IV) hexanitrato dianions and a free analogue of dicationic anion-exchange sites correlate well with empirically-determined distribution coefficients. This Quantitative Structure Activity Relationship (QSAR) is useful in the determination of the overall trend within a select series of bifunctional resins and which structural modifications are most likely to be adventageous. Ultimately, we hope to refine this methodology to allow the *a priori* determination of ion-exchange behavior for a broad class of materials.

RECEIVED
DEC 13 2000
OSTI

Introduction

Anion exchange in nitric acid is a frequently used process for the recovery of plutonium from a wide range of impure materials. The large coordination sphere (up to 12 coordinate) of plutonium enables it to form anionic complexes in high nitrate media where few other metals form competing anionic species. Spectroscopic studies of plutonium (IV) in nitric acid solution and sorbed to ion-exchange media indicate that the species sorbed onto anion exchange resins is the di-anionic hexanitrato complex.[1] This unique chemical behavior is exploited by the anion-exchange process used in the Plutonium Facility at Los Alamos National Lab. Plutonium recovery operations in nitric acid currently use Reillex HPQ® (Reilly Industries) a macroporous polymer of N-methylated 4-vinylpyridine crosslinked with divinylbenzene.

Under typical anion-exchange conditions, sorption of a dianionic species requires complexation to two separate cationic resin sites. The orientation and availability of these sites for cooperative interactions with a dianion is not well controlled. We have synthesized and evaluated several series of bifunctional resins where the structure of the anion-receptor site is well defined. These resins are synthesized via N-derivatization of pyridinium units from a base poly(4-vinylpyridine) resin with a second cationic site such that the two anion-exchange sites are linked by 'spacer' arms of varying length and flexibility. Three series of bifunctional resins are presented in Figure 1. Plutonium sorption data from nitric acid media has been reported for these materials,[2] and distribution data indicate that the controlled geometry of the anion-exchange sites has a positive impact upon the sorption of the actinide dianion.

(Figure 1)

Modeling the interactions of actinide hexanitrato complexes with the dicationic resin sites is a complex, multi-stage process. We report herein the modeling of the electrostatic interactions of the plutonium hexanitrato dianion with analogues of the resin dicationic sites for three series of resins. We have developed a parameter called the Stickiness Factor (SF) which we correlate with experimental distribution coefficients. The Stickiness Factor is defined as the sum of the intermolecular electrostatic moments and is calculated herein using partial and formal charges for the energy-minimized structure of each ion pair. Empirical correlation between the calculated SF and the experimentally-determined distribution coefficients for plutonium uptake is good and strongly suggests that this methodology can be further developed in the future to allow *a priori* predictive capabilities.

Experimental

Computational approach

Although any individual $Pu(NO_3)_6^{2-}$ moiety docks and undocks with the cationic sites of the anion-exchange resin repeatedly, we can consider this process to be a single docking operation in that one complex has moved from the solution phase onto a solid phase in the macroscopic sense. In this docking procedure, there are many forces at work (*i.e.* electrostatics, geometry constrants (sterics), London forces, entropy forces, cavitation, phase change enthalpies, dispersion forces, etc.), but our model considers only electrostatic and steric forces. Electrostatics are the dominant attractive force between the $Pu(NO_3)_6^{2-}$ complex and the pyridium-based dication. While 5-f orbitals are extremely important *within* the $Pu(NO_3)_6^{2-}$ complex, they are not a factor in intermolecular interactions since their radial distribution beyond 6 Å is negligible[3] and molecular modeling using HyperChem[4] predicts the closest intermolecular Pu-H distance to be ~5 Å and Pu-C or Pu-N to be over 6 Å. Steric interactions are considered to be the primary intra-and intermolecular repulsive forces.

Experimentally-determined plutonium distribution coefficients (K_d's) were measured and calculated by contacting 6 mL of 3 mg/mL Pu(IV) in 1-9 M nitric acid with 250 mg of resin.[2] We selected the K_d values for 9$\underline{M}$ HNO_3 (the acid concentration where the plutonium sorption is maximized) taken at 30 minutes for our correlations and comparisons discussed below. Although the measurements taken at 30 minutes do not reflect true equilibrium conditions, the experimental K_d values determined at longer times are so large as to have unmanageably large uncertainties (+/- 50-100%). Distribution coefficients may be compared directly with equilibrium constants (K_{eq}) in that both reduce to the ratio of bound to free plutonium multiplied by constants.[5] Correlation of our SF with ΔH and other components of equilibrium constants is underway and is slated for future publication.

Computational Methods

The use of formal-charge metrics to describe charge distribution within a molecule is as inaccurate as it is simple. However, the use of formal charges in the calculation of intermolecular attraction is reported herein due to one of our continuing goals - to bring computational resources to the bench chemist. For the plutonium hexanitrato dianion, non-zero charges were assigned as follows: Pu (+4), N(+1), O(-0.66). For the dications, only nitrogen (+1) was assigned a charge.

In addition to the use of basic formal-charge metrics, we calculated partial-charge distributions in an attempt to provide a more accurate model of the electrostatic interactions between actinide hexanitrato anions and cationic substrates. PM3 microstate configuration interaction (CI) calculations involving two occupied and two unoccupied orbitals at the MM+ optimized geometry using HyperChem 5.1[4] calculates a charge of +0.8 e for the nitrogen atoms. While this charge fits with the formal-charge methodology, nitrogen is the most electronegative atom within the dication. Therefore, we were not satisfied with these charge distribution results. Unfortunately, both *ab initio* MCSCF calculations and more basic CI calculations were inaccessible due to the large number of atoms (30 to 50 atoms). We concluded that an *ab initio* GAMESS[6] ROHF single-point energy calculation run on an IBM RS6000/590 with the MIDI basis set at the MM+ optimized geometry was appropriate to model the partial-charge distribution for two of the three dication systems. We choose Mulliken charges, although similar accuracy can be obtained with Lowdin charges. We determined that the MIDI basis set was too small to properly describe the d-orbital atoms of the trimethylphosphine dications, $C_5H_5N(CH_2)_xP(CH_3)_3^{2+}$, so partial charge distributions are not currently reported for this system. A list of partial charge by atom for the dications is available as supplementary material.

Ab initio calculations for the entire plutonium hexanitrato dianion are also exceedingly tedious because the complex is large (25 atoms) and suffers from intractable orbital degeneracy. We developed a theoretical neutral 'compound', the triradical $Pu(NO_3)^{\cdots}$, which has a multiplicity of 8. This model can be optimized with either ROHF or RHF methods. The seventy-eight core electrons of the plutonium are replaced by relativistic effective core potentials (RECP's).[7] Use of RECP's for plutonium disallows the use of RECP's for the other atoms. The Hückel subroutine in GAMESS has not been coded for 5-f orbitals, so diagonalization of the one electron Hamiltonian (an HCORE guess) was used to start the calculation. This model complex converges readily and yields the following partial charge metrics. The two oxygens bound to the Pu(IV) are -0.50 e, the nitrogen atom is +0.58 e, and the outside oxygen is -0.35 e. Thus, each nitrato ligand contributes 0.77 electron to the complex, yielding a net partial charge of +2.62 e for the Pu(IV) center of the $Pu(NO_3)_6^{2-}$ complex.

Optimized anion/cation configurations are determined using HyperChem's MM+ on a dual Pentium Pro 200. MM+ is very efficient in modeling sterics and has been shown to be reasonably fast and accurate at modeling both actinide complexes and organic systems.[8] The optimized ion-pair configuration was selected from energy-minimized structures generated from various initial configurations. The sum of the forces between the ions (SF) was calculated using partial or formal charge metrics as described below. While this sum does not directly reflect changes in bond-strain energies associated with the ion pairing, they are accounted for indirectly because bond-strain is a determining factor in the conformation of the energy-minimized ion-pair. Figure 2 presents an energy-minimized interaction between the plutonium hexanitrato dianion and the free analogue of the resin with a butylene spacer and trimethylammonium terminus.

(Figure 2)

Summing all the electrostatic effects between all the atoms in intermolecular systems was done *via* dynamic data exchange (DDE) with Microsoft's Visual C++ 5.[9] In equation 1, the Stickiness Factor (SF) is defined as the sum of the intermolecular electrostatic moments where *i* and *k* are the molecule index, *j* and *l* are the atoms inside molecule *i* and *k* respectively (as assigned by HyperChem), *q* is the charge on the atom, and *r* is the distance from atom(*i,j*) to atom(*k,l*) in Å. The cartesian coordinates for all of the monomers are available in the supplementary materials.

$$SF \equiv \frac{1}{2} \sum_{i \neq k} \frac{q(i,j) \cdot q(k,l)}{r((i,j)(k,l))} \qquad eq.1$$

Stickiness Factor values for ion pairs calculated using partial and formal charge metrics is presented in Table 1. When using formal-charge metrics, summation of the electrostatic charge interactions is greatly simplified by the number of atoms with zero charge.

(Table 1)

Results and Discussion

Correlation of SF with K_d for the corresponding resin was determined by plotting the experimental K_d values versus the calculated SF values for each ion pair within a series, then applying a simple linear fit (Figure 3). While thermodynamic equations predict an exponential fit ($K_d = e^{-\Delta G/RT}$), e to a very small number is essentially linear. Linear correlation coefficients (r) were similar for ln K_d vs. SF and K_d vs. SF plots. The correlation between SF and K_d has a negative slope, reflecting the hypothesized relationship between the force of electrostatic attractions (a more negative value indicates a stronger attractive force) and the affinity of the dicationic site for the plutonium hexanitrato dianion (a more positive K_d indicates greater plutonium uptake from solution). Correlation values were reported herein as r^2.

(Figure 3)

Calculated K_d values are derived from the empirical linear correlation. It is, admittedly, a circular process and, at this point, only an alternative way of viewing the goodness-of-fit and of extrapolating predicted K_d values to a longer spacer group than we currently have experimental data to support. An *a priori* determination of K_d values from the SF values between series of resins would require knowing the slope and intercept for each type of functional group - a capability we have not yet developed. The intercept value is most probably related to the magnitude of the TdS term of ΔG, and we will continue to pursue methods for determination of this term. However, the straightforward determination of *which* member of a *series* would display the best distribution values can be extracted directly from the SF values.

For the $[C_5H_5N(CH_2)_xC_5H_5N]^{2+}$ series (x = 2,3,5,6), the QSAR correlation using formal-charge metrics predicts a trend which is very similar to the experimental results ($r^2 = 0.97$), Figure 4. Only four data points (x = 2, 3, 5, 6) where used in the correlation since data for the x = 4 resin data is unavailable. The calculated K_d for the hexylene spacer is slightly greater than for the pentylene spacer, a reversal from the experimental results, but the rest of the series is in the same order as found experimentally. Use of partial-charge metrics marginally improves the correlation ($r^2 = 0.98$) between SF and experimental distribution coefficients. The overall trend correlates well with the experimental data (5 > 6 > 3> 2). Both methods predict that the high degree of angle strain and steric hindrance within the dicationic site for the unit with an ethylene spacer should correlate with a low experimental K_d observed for the corresponding resin.

(Figure 4)

As seen in Figure 5 and Table 1, formal-charge metrics predict an overall trend in distribution behavior for the $C_5H_5N(CH_2)_xN(CH_3)_3^{2+}$ series (x = 2 - 6) which generally falls in the same order as is found experimentally. The ordering of the propylene and pentylene spacers is reversed, but the calculated values are well within the experimental uncertainty. It is interesting to note even this extremely simplified scheme correctly determines that the resin with a butylene spacer would be the best and the resin with a hexylene spacer to be the worst.

The correlation for the $C_5H_5N(CH_2)_xN(CH_3)_3^{2+}$ series using partial-charge metrics is less satisfactory. One notable difference is that the SF calculation predicts that the dication with the propylene spacer would display the highest K_d value. However, calculated values for x=2-5 are all relatively close and are still well within the uncertainty of the experimental data. Both models predict that spacer lengths longer than x=6 will dramatically diminish affinity for the plutonium complex.

(Figure 5)

For the $C_5H_5N(CH_2)_xP(CH_3)_3^{2+}$ series (x = 2 - 5), this formal-charge method predicts the same sequencing as found experimentally (5 > 4 > 3 >> 2), Table 1 and Figure 6. The quality of the fit is similar to the previous two systems ($r^2 = 0.86$). The SF calculations for this system predict that the plutonium complex affinity for the system with a hexylene spacer would be extremely weak, and the empirical correlation with experimental data produces an unrealistic negative K_d value. This unusual response is, at least in part, an artifact of shallow slope of the linear fit and few data points.

(Figure 6)

Conclusion

Recent studies of bifunctional cation/anion interactions in systems selected for strain-free contact showed an disadvantage of only about 0.5 kJ mol^{-1} in free energy for each additional akylene unit between sites.[10] This value is significantly lower than would be expected from entropic considerations alone, so it was concluded that entropic disadvantages could be offset by enthalpic advantages such as a slightly better fit with more flexible systems. Our studies support these conclusions in that each series of dicationic resins, where the two cationic sites are separated by alkylene spacers of varying length, exhibit a distinct correlation between the experimentally-determined affinity with the plutonium hexanitrato dianion and the calculated electrostatic interactions within the energy-minimized structure. The molecular mechanics-based calculations used here predict that systems with alkylene spacers longer than needed for an optimized dication/dianion interaction will exhibit progressively decreased anion affinity, primarily due to increased bond strain and entropic effects.

For the formal-charge systems, MM+ structural optimization and calculation of the SF was computed within 15 minutes per ion-pair on a personal computer running readily available softeware. Even though the formal-charge model is simplistic, it is quite reasonable at predicting the overall trends within each series of resin. In general, both the partial- and formal-charge models predict that the 3-4 methylene spacer is optimal, while experimentally we find that the highest K_d values are with resins containing a 4-5 methylene spacer between cationic sites. Both methodologies predict a rapid decrease in expected performance for longer spacers (x >6) which we have not confirmed experimentally.

Due to the thermodynamic approximations used here, we cannot predict a K_d for a single resin structure and are restricted to determining the overall trends inside a family of related materials. The SF methodologies presented here implicitly contain the assumption that the phase-change enthalpies and entropic forces are constant within a series of resins. We are presently investigating ways to unravel the finer energy contributions required to better understand the docking and to understanding how a better description of these molecules will effect the partial charge calculations. It is somewhat annoying that the simplistic formal-charge QSAR method is just as reliable at predicting behavior as the more complex, and presumably more realistic, partial-charge model.

We anticipate that this QSAR method can become very useful in sorting potential structures, thereby reducing the time and cost associated with synthesizing and evaluating less viable candidates. We plan to continue to refine our calculations to include additional parameters and to gather more experimental data for correlation with theoretical modeling data.

References

[1] a) J. L. RYAN, E. J. WHEELWRIGHT, The Recovery, Purification and Concentration of Plutonium by Anion Exchange in Nitric Acid, U.S. Atomic Enery Commission report TID-7606, 1960, and b) S. F. MARSH, R. S. DAY, D. K VEIRS, Spectrophotometric Investigation of the Pu(IV) Nitrate Complex Sorbed by Ion Exchange Resins, Los Alamos National Laboratory report LA-12070 (June 1991).

[2] S. F. MARSH, G. D. JARVINEN, R. A. BARTSCH, Reactive Polymers, 35 (1997) 75.

[3] A J. FREEMAN AND G. H. LANDER, editors, Handbook on the Physics and Chemistry of the Actinides,vol. 1, North-Holland: Amsterdam (1984).

[4] HyperChem ver. 5.1, Hypercube, Inc., 1115 NW 4th Street, Gainesville, Florida 32601, USA.

[5] F. HELFFERICH, Ion Exchange, Dover Publications, Inc., New York (1995).

[6] M. W. SCHMIDT, K. K. BALDRIDGE, J. A. BOATZ, J. H. JENSEN, S. KOSEKI, N. M. MATSUNAGA, M. S. GORDON, K. A. NGUYEN, S. SU, T. L. WINDUS, S. T. ELBERT, J. Comput. Chem., 14 (1993) 1347.

[7] W. C. ERMLER, R. B. ROSS, P. A. CHRISTIANSEN, J. Quantum Chem., 40 (1991) 829.

[8] N. L. ALLINGER, U. BURKET; Molecular Mechanics, ACS monograph series 177, American Chemical Society, Washington, DC (1982).

[9] Microsoft Visual C++; Professional ed., ver. 5, Microsoft, Redmond, WA (1997).

[10] M. A. HOSSAIN, H-J SCHNEIDER, Chem. Eur. J., 5 (1999) 1284.

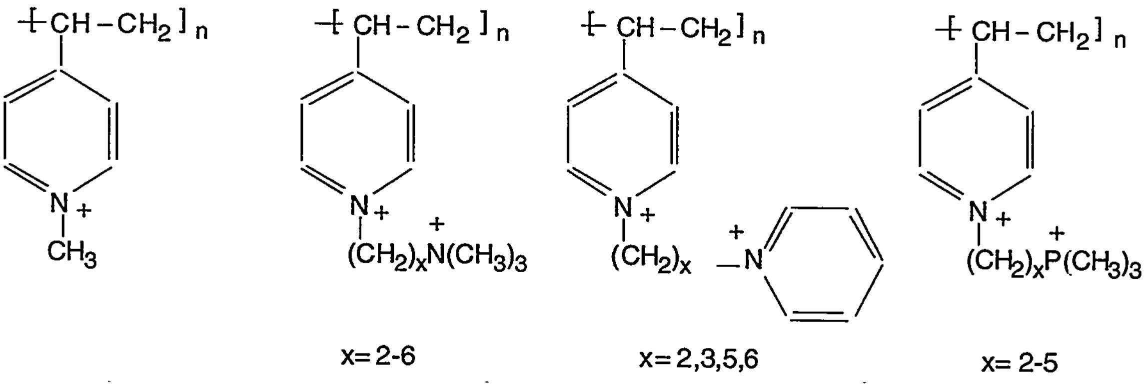

Figure 1. Methylated (Reillex HPQ®) and experimental bifunctional resins.

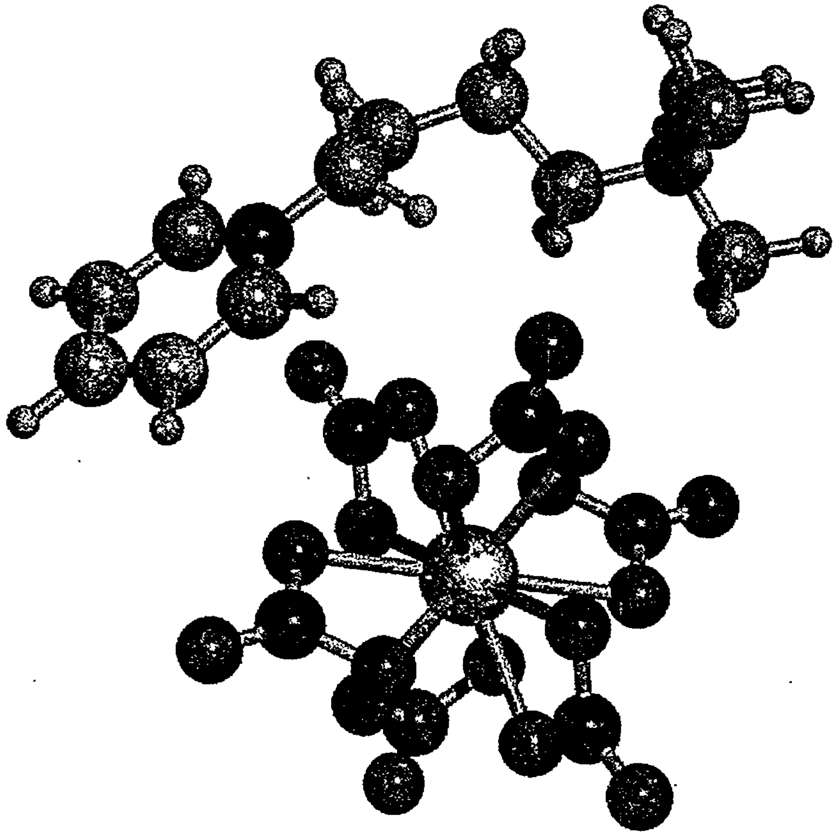

Figure 2. Energy-minimized structure of the plutonium hexanitrato dianion with a free analogue of the pyridinium-based resin with a butylene spacer and a trimethylammonium cationic site.

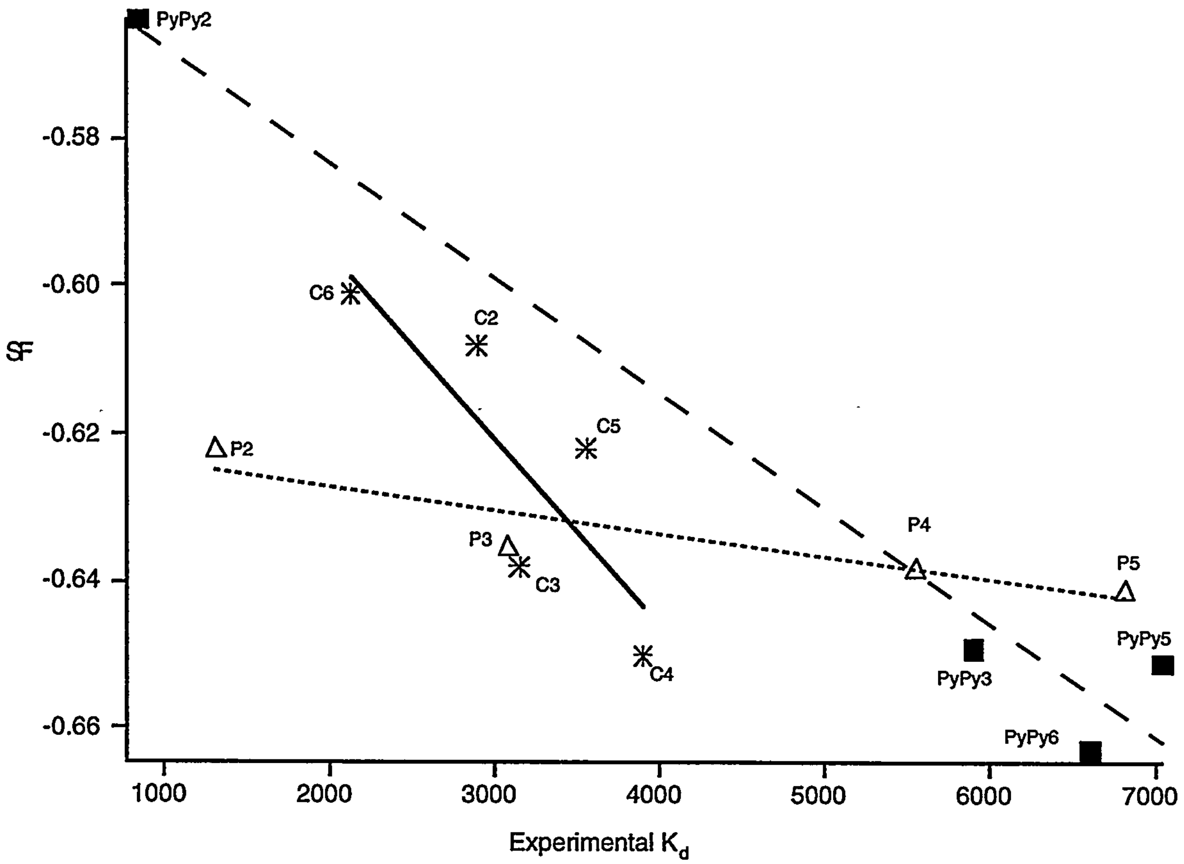

Figure 3. Stickness factor (SF) versus experimental Pu(IV) distribution coefficients (K_d) for ion pairs for three series of dications using formal charge metrics. Dication names are abbreviated as follows: Cx is $[C_5H_5N(CH_2)_xN(CH_3)_3]^{2+}$ (solid line), Px is $[C_5H_5N(CH_2)_xP(CH_3)_3]^{2+}$ (dotted line), and PyPyx is $[C_5H_5N(CH_2)_xC_5H_5N]^{2+}$ (dashed line).

$[C_5H_5N(CH_2)_xC_5H_5N]^{2+}$

		Formal Charge Model			Partial Charge Model		
	exp. K_d	SF	calc. K_d	% Δ	SF	calc. K_d	% Δ
x = 2	850	-0.564	904	6	-0.538	840	1
x = 3	5900	-0.649	6200	5	-0.614	6400	8
x = 4	-	-0.638	5500	-	-0.619	6800	-
x = 5	7000	-0.651	6300	10	-0.616	6600	6
x = 6	6600	-0.663	7000	6	-0.615	6500	2
x = 7	-	-0.620	4400	-	-0.598	5300	-
			r^2= 0.97			**r^2= 0.98**	

$C_5H_5N(CH_2)_xN(CH_3)_3^{2+}$

		Formal Charge Model			Partial Charge Model		
	exp. K_d	SF	calc. K_d	% Δ	SF	calc. K_d	% Δ
x = 2	2900	-0.608	2700	-7	-0.614	3200	10
x = 3	3200	-0.638	3500	9	-0.621	3600	13
x = 4	3900	-0.650	3900	0	-0.620	3500	-10
x = 5	3600	-0.622	3100	-14	-0.612	3100	-14
x = 6	2100	-0.601	2500	19	-0.593	2200	5
x = 7	-	-0.575	1700	-	-0.564	800	-
			r^2=0.70			**r^2= 0.68**	

$C_5H_5N(CH_2)_xP(CH_3)_3^{2+}$

		Formal Charge Model			Partial Charge Model		
	exp. K_d	SF	calc. K_d	% Δ	SF	calc. K_d	% Δ
x = 2	1300	-0.622	910	-29	-	-	-
x = 3	3100	-0.635	4400	45	-	-	-
x = 4	5500	-0.638	5300	-4	-	-	-
x = 5	6800	-0.641	6100	-10	-	-	-
x = 6	-	-0.614	-1300	-	-	-	-
			r^2=0.86				

Table 1. Calculated SF values, experimental and calculated K_d values for the three series of resins.

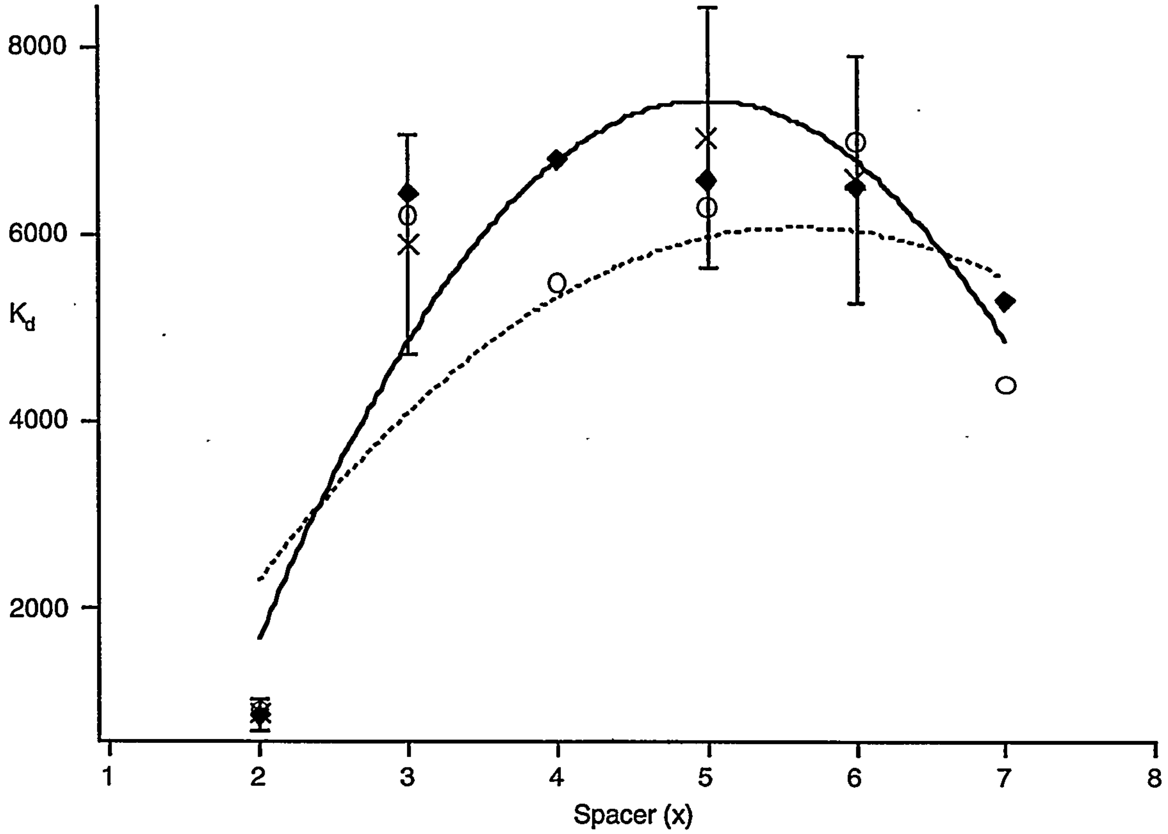

Figure 4. Experimental and predicted K_d for $[C_5H_5N(CH_2)_xC_5H_5N]^{2+}$ as a function of akylene spacer length using partial (_) and formal (_) charges. Experimental data (_) is represented with 20% uncertainty bars. Solid and dashed curves are a graphical representation of the predicted trends in the distribution coefficients for the partial- and formal-charge models, respectively.

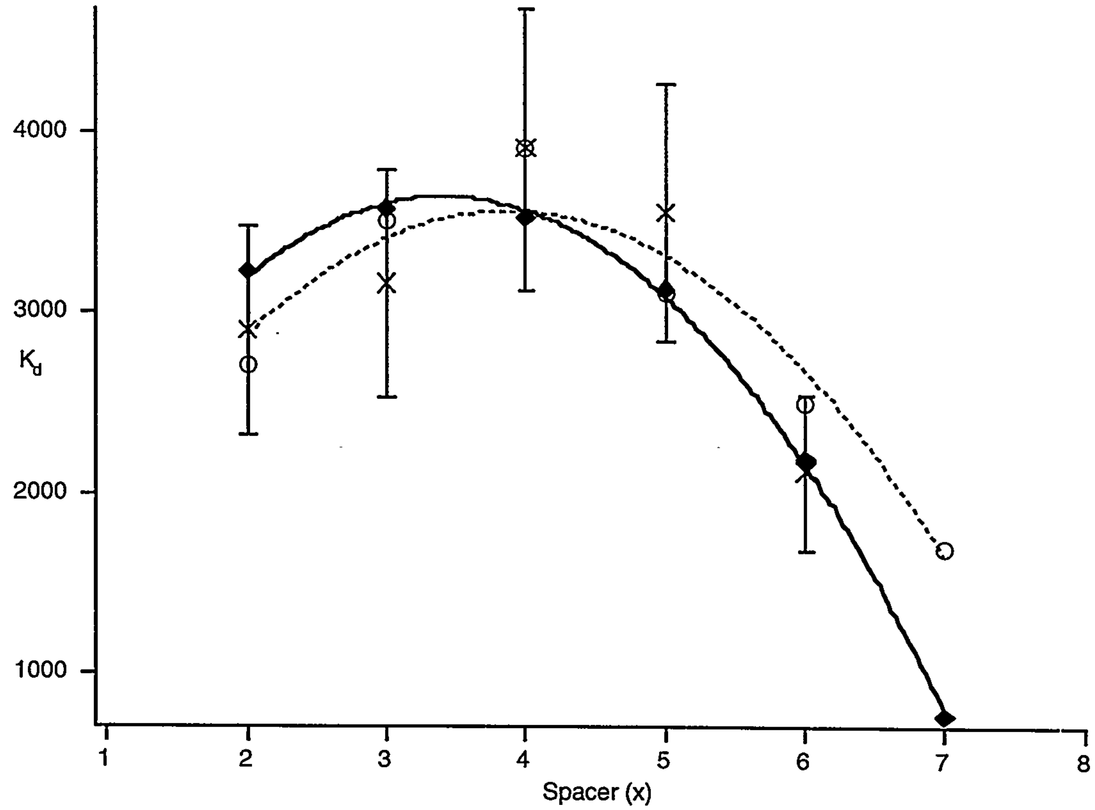

Figure 5. Experimental and predicted K_d for $C_5H_5N(CH_2)_xN(CH_3)_3^{2+}$ as a function of alkylene spacer length using partial (_) and formal (_) charges. Experimental data (_) is represented with +/- 20% uncertainty. Solid and dashed curves are a graphical representation of the predicted trends in the distribution coefficients for the partial- and formal-charge models, respectively.

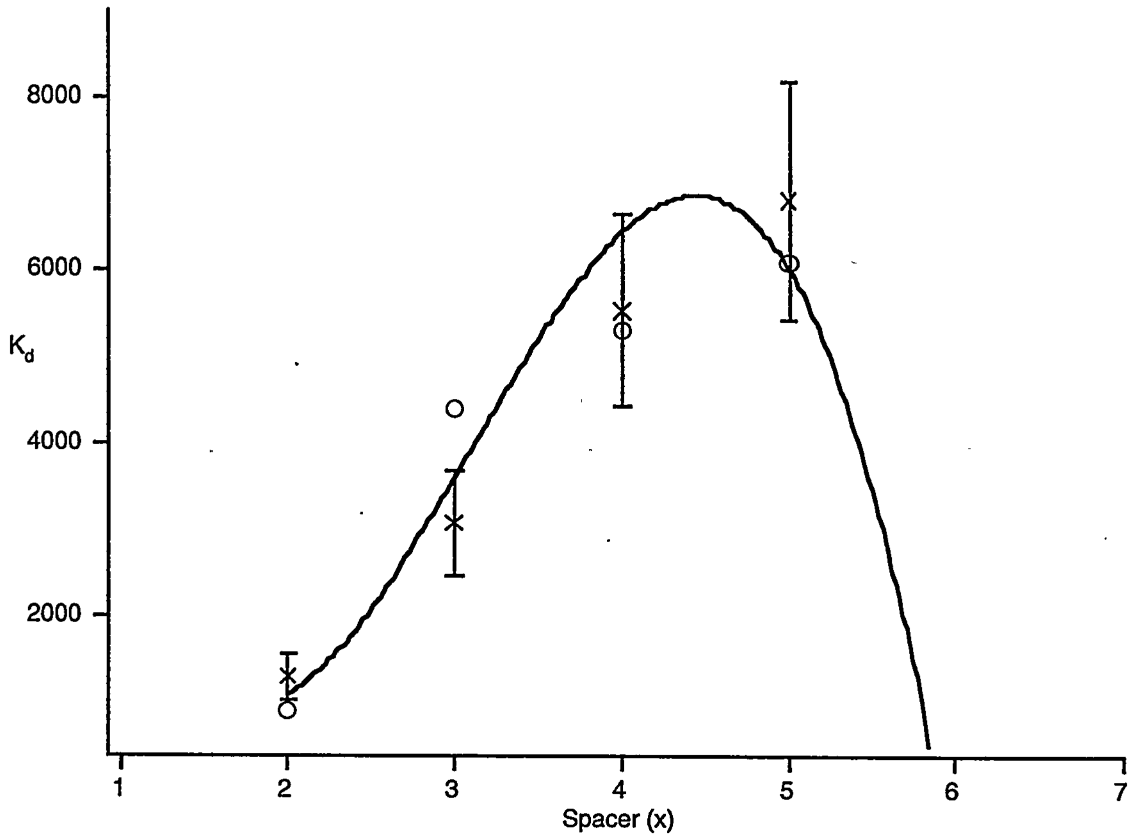

Figure 6. Experimental and predicted K_d for $C_5H_5N(CH_2)_xP(CH_3)_3^{2+}$ as a function of alkylene spacer length using formal (_) charges. Experimental data (_) is represented with +/- 20% uncertainty. The solid curve is a representation of the predicted trend in the distribution coefficients.